Physics underlying controlled self-assembly of micro- and nanoparticles at a two-fluid interface using an electric field

Nadine Aubry

Department of Mechanical Engineering, Carnegie Mellon University, Pittsburgh, Pennsylvania 15213, USA

Pushpendra Singh

Department of Mechanical Engineering, New Jersey Institute of Technology, Newark, New Jersey 07102, USA

The purpose of this paper is to investigate the physics underlying the controlled self-assembly of microparticles and nanoparticles at a two-fluid interface using an electric field. As shown in recent experiments, under certain conditions an externally applied electric field can cause particles floating at a two-fluid interface to assemble into a virtually defect free monolayer whose lattice spacing can be adjusted by varying the electric field strength. In this work, we assume that both fluids and particles are perfect dielectrics and for this case analyze the (capillary and electrical) forces acting on the particles, deduce an expression for the lattice spacing under equilibrium condition, and study the dependence of the latter upon the various parameters of the system, including the particles' radius, the dielectric properties of the fluids and particles, the particles' position within the interface, the particles' buoyant weight, and the applied voltage. While for relatively large sized particles whose buoyant weight is much larger than the vertical electrostatic force, the equilibrium distance increases with increasing electric field, for submicron sized particles whose buoyant weight is negligible, it decreases with increasing electric field. For intermediate sized particles, the distance first increases and then decreases with increasing electric field strength.

I. INTRODUCTION

A technique in which an electric field is applied in the direction normal to a two-fluid interface has been recently developed to control the process of particles self-assembly at the interface [1,2]. Particles floating at an interface, in general, self-assemble or cluster because they deform the interface, thus giving rise to lateral capillary forces which cause the particles to cluster. For example, cereal flakes floating on the surface of milk cluster by this mechanism. The attractive lateral capillary forces arise due to the fact that for two floating particles, the deformed interface is such that the interface height between the particles is lowered due to the interfacial tension [3]. It is easy to see that the lateral component of the capillary force acting on the particles is attractive and causes them to move toward each other.

This naturally occurring phenomenon, however, produces monolayers that display many defects, lack order (both short and long ranged) and whose distance between the particles cannot be controlled, three drawbacks which seriously limit the range of applications one can target using this technique. In addition, such a phenomenon does not manifest itself on particles smaller than ∼10 μm. The technique developed in Refs [1,2] overcomes all these shortcomings (see Fig. 1). The clustering of particles at interfaces is important because it is capable of modifying the interfacial properties of two-phase systems and also because it is used for the self-assembly of particles to form monolayers at two-liquid interfaces (see Ref. [4], and references therein).

In equilibrium, the vertical position of a floating particle within a two-fluid interface is such that the sum of the forces acting on the particle in the direction normal to the interface is zero. A particle denser than the liquid below can float on

its surface because the vertical component of the capillary force, which arises due to the deformation of the interface, balances the particle's buoyant weight (see Fig. 2). For a small particle of radius a, the buoyant weight, which scales as a^3, becomes negligible, and therefore only a small interfacial deformation is needed in this case for the vertical capillary force to balance the buoyant weight. Consequently, the lateral capillary forces due to this small deformation of the interface are too small to move micron and nanosized particles, and thus, small particles, in general, do not self-assemble. It is known that for particles floating on the air-water interface the attractive capillary forces are significant only when the particle radius is larger than ∼10 μm [4]. This restriction, however, does not apply to particles trapped

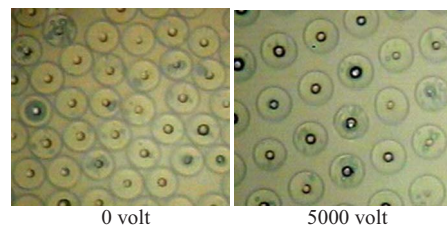
FIG. 1. (Color online) Assembly of glass particles floating at an air-oil interface. The average radius of the particles is 23.5 μm. (a) Particles self-assemble under the action of the lateral capillary forces alone. The lattice is approximately triangular, but lacks long range order and contains many defects. (b) When a voltage V =5000 V is applied, particles move away from each other and form a defect-free triangular lattice in which the distance between the particles is approximately 2.7 times the particle radius. This order is maintained as the electric field is either increased or decreased, particularly as it is decreased to zero [1].
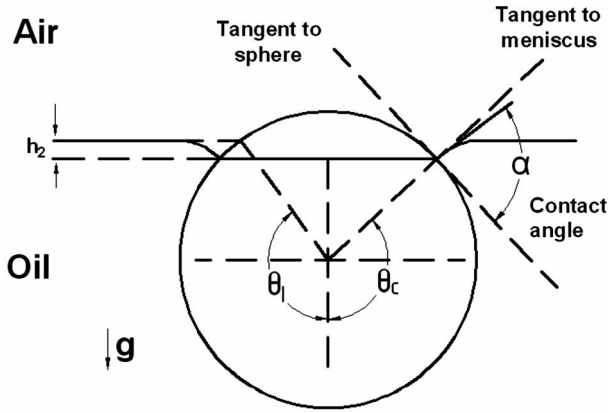
FIG. 2. Schematic of a heavier than liquid hydrophilic (wetting) sphere of radius a hanging on the contact line at θ_c. The point of extension of the flat meniscus on the sphere determines the angle θ_1 and h_2 is defined as $h_2 = a(\cos\theta_c - \cos\theta_1)$. The angle α is fixed by the Young-Dupré law and θ_c by the force balance.

in thin films with a thickness smaller than the particle diameter. In fact, particles ranging from protein macromolecules to millimeter sized particles can self-assemble in such thin films [5]. Moreover, small particles can self-assemble if they are charged or if they have irregular contact lines [6].

Experiments described in Ref. [1] show that particles floating at a two-fluid interface can be self-assembled to form monolayers by applying an electric field normal to the interface, and that the lattice spacing of the monolayers thus formed can be adjusted by varying the electric field strength. The technique also leads to the formation of virtually defect free monolayers with long-range order and, in principle, can be used for manipulating the assembly of submicron sized particles in two-fluid interfaces. It thus overcomes all the shortcomings of the usual capillarity induced clustering mentioned earlier.

We next discuss the dependence of the electrostatic force acting on a particle upon the parameters of the system such as the dielectric constants of the fluids and particles, the particles' position within the interface, and the distance between the particles. It is also shown that the component of the electrostatic force normal to the interface alters the deformation of the interface due to the particles, and thus the magnitude of the lateral capillary forces. The lateral component of the electrostatic force acting on the particles is repulsive, and its balance with the attractive capillary force is used to determine the equilibrium distance between the particles. It is assumed that both the particles and the fluids considered here are perfect dielectrics.

II. ELECTROSTATIC FORCES, GOVERNING EQUATIONS, AND DIMENSIONLESS PARAMETERS

As in the case of our experiments, it is assumed that the electric field away from the interface is uniform and normal to the undeformed interface (see Fig. 3). It is well known that while an isolated uncharged dielectric particle placed in a uniform electric field becomes polarized, it does not experience any electrostatic force. This, however, is not the case
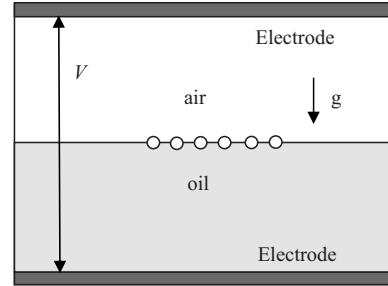

FIG. 3. Schematic of the experimental setup used in Ref. [1] to assemble particles on the surface of corn oil. The distance between neighboring particles is controlled by adjusting the magnitude of the applied voltage. An ac electric field with frequency 100 Hz was used to make the influence of conductivity negligible.

for a particle floating at a two-fluid interface because of the mismatch between the dielectric constants of the two fluids involved. Moreover, from symmetry it is clear that the electrostatic force acting on an isolated spherical particle at an interface can only be in the direction normal to the interface, but depending on the parameter values it can be either upward or downward. If the particle is charged, a Coulomb force also acts on the particle. In addition, when there are other particles present at the interface they interact with each other via dipole-dipole interactions. We now proceed to compute the electrostatic force acting on the particles at the interface, first briefly describing the numerical method used.

A. Numerical method

Let us denote the domain containing the two fluids and spherical particles (of identical radii and properties) by Ω, the interior of the ith particle and its surface by $P_i(t)$ and $\partial P_i(t)$, respectively, and the domain boundary by Γ. To calculate the electric field $\mathbf{E}$, we first solve the electric potential problem for ϕ in Ω, namely, $\nabla \cdot (\epsilon \nabla \phi) = 0$ subjected to the boundary conditions on the particle surfaces and the two-fluid interface. On the particle surface $\partial P_i(t)$, the conditions read $\phi_1 = \phi_2$, $\epsilon_c \partial \phi_1 / \partial n = \epsilon_p \partial \phi_2 / \partial n$ where ϕ_1 and ϕ_2 are the electric potentials in the liquid and particle, and ϵ_c and ϵ_p are the dielectric constants of the fluid and particle. A similar boundary condition is applied at the two-fluid interface. The electric potential is prescribed on the electrodes as constant values and the normal derivative of the potential is taken to be zero on the remaining domain boundary. The electric field is then deduced from the equation $\mathbf{E} = -\nabla \phi$. The Maxwell stress tensor $\boldsymbol{\sigma}_M$ is given by $\boldsymbol{\sigma}_M = \epsilon \mathbf{E}\mathbf{E} - 1/2\,\epsilon(\mathbf{E} \cdot \mathbf{E})\mathbf{I}$, where $\mathbf{I}$ is the identity tensor and the electrostatic force acting on the ith particle is then obtained by integrating $\boldsymbol{\sigma}_M$ over its surface, i.e., $\mathbf{F}_{\mathrm{DEP}} = \int_{\partial P_i(t)} \boldsymbol{\sigma}_M \cdot \mathbf{n}\,d\mathbf{s}$, where $\mathbf{n}$ is the unit outer normal on the surface of the ith particle. The computational domain in our finite element code is discretized using a tetrahedral mesh and the boundary conditions are imposed on the surface of the particles. The resulting linear system of equations is solved using a multigrid preconditioned conjugate gradient method [7].

B. Vertical electrostatic force

As noted above, even though the applied electric field away from the interface is uniform, a particle within the

interface experiences an electrostatic force normal to the interface due to a jump in dielectric constants across the interface. If the interface does not contain any particles, the electric field is normal to the interface and its intensity in the lower and upper fluids is constant, while changing discontinuously at the interface according to the boundary condition stated above.

In the case of two spherical particles placed at the interface, the electric field distribution on the domain mid plane, which passes through the spheres centers, is shown in Fig. 4 for three different combinations of dielectric constants when the particle centers are at the undeformed interface. To compute the electrostatic force acting on the particles, we must first determine the shape of the interface which, in general, is deformed due to the presence of the particles. The deformed interface shape can be computed by solving the equations of motion for the fluids and the particles and for the interface, subjected to the contact angle and boundary conditions. This, however, is difficult to do analytically and beyond the scope of this manuscript. The dielectric constant of the upper fluid is assumed to be 1, while those of the lower fluid and the particles are varied. The figure shows how the particles presence at the interface modifies the electric field distribution. In particular, the electric field is the weakest in the fluid or particle region in which the dielectric constant is the largest and the strongest in the region for which the dielectric constant is the smallest. For example, in Fig. 4(a), where the dielectric constant of the particles has a value in between the dielectric constants of the lower and upper fluids, the electric field intensity is the strongest in the upper fluid, the weakest in the lower fluid and in between these two values inside the particles. It follows that the magnitude of the vertical electrostatic force on the particle, as well as its direction, depends on the dielectric constant values. For example, the force is positive (acts against gravity) in Figs. 4(a) and 4(b), and negative in Fig. 4(c). The lateral electrostatic force is repulsive in all three cases, but its magnitude depends on the dielectric constant values and is different for the three cases.

We now turn to the electric field distribution around a particle when its position within the interface is altered (Fig. 5). Notice that because of the presence of the interface the electric field around the particles is not symmetric and, as a result, the particle experiences an electrostatic force in the direction normal to the interface. For these calculations, the dielectric constants of the upper fluid, the lower fluid and the particle are set to $\epsilon_a = 1.0$, $\epsilon_L = 5.0$, $\epsilon_p = 0.5$. Figure 5(a) shows that a particle with its center at the undeformed interface experiences an electrostatic force in the upward direction. The electric field distributions for the cases when the particle center is below and above the undeformed, flat interface are shown in Figs. 5(b) and 5(c). The electrostatic force is in the upward direction in the former case and in the downward direction in the latter case.

Our numerical results show that the vertical component of the electrostatic force in a dc field (or time averaged force in an ac field) acting on a particle can be written as

$$F_{\text{ev}} = a^2 \epsilon_0 \epsilon_a \left(\frac{\varepsilon_L}{\varepsilon_a} - 1 \right) E^2 f_v \left(\frac{\epsilon_L}{\epsilon_a}, \frac{\epsilon_p}{\epsilon_a}, \theta_c, \frac{h_2}{a} \right). \quad (1)$$

Here a is the particle radius, $E = V_0/L$ is the average electric field strength away from the particle (or the r.m.s. value of

the electric field in an ac field), ϵ_p, ϵ_a, and ϵ_L are the dielectric constants of the particle, the upper fluid and the lower fluid, respectively, and $\epsilon_0 = 8.8542 \times 10^{-12}$ F/m is the permittivity of free space. Here, L is the distance between the electrodes, V_0 is the voltage difference applied to the electrodes, and $f_v(\epsilon_L/\epsilon_a, \epsilon_p/\epsilon_a, \theta_c, h_2/a)$ is a dimensionless function of the included arguments (θ_c and h_2 being defined in Fig. 2). The dependence of the force on the particle radius a is quadratic which was established numerically as shown in Fig. 6. The factor $(\epsilon_L/\epsilon_a - 1)$ ensures the fact that the force is zero when $\epsilon_L/\epsilon_a = 1$ as the fluids dielectric constants are the same in this case. It is assumed that the interface is flat and intersects the particle's surface at θ_c (see Fig. 2). One of the focuses of this paper is on the behavior of small floating particles for which the interfacial deformation is negligible, and thus $\theta_c \approx \pi - \alpha$, where α is the contact angle (see Fig. 2). In addition, the influence of electrowetting is considered only in the sense that if there is a change in the effective contact angle, the resulting change in the particle's position within the interface can be accounted for by changing θ_c [8]. Also notice that the dependence of the electrostatic force on the particle radius a is quadratic compared to the cubic dependence of the dielectrophoretic force which acts on a particle in a nonuniform electric field.

In Fig. 7, we have set $\epsilon_a = 1$, and $\epsilon_p = 2.0$ [Fig. 7(a)] or 0.5 [Fig. 7(b)], and studied the force coefficient f_v as a function of $\sin \theta'_c$ for various values of ϵ_L, where $\theta'_c = \theta_c - \pi/2$. Notice that it is sufficient to consider the case where $\epsilon_L > \epsilon_a$ because the electric force for the corresponding case where $\epsilon_L < \epsilon_a$ can be deduced from the results shown in Fig. 7 by simply reversing the direction of the force. The figure shows that for $\sin \theta'_c < 0$ the force coefficient f_v is positive for all cases investigated here and its magnitude decreases with increasing ϵ_L. A positive value of the electrostatic force for $\theta'_c < 0$ implies that the particle is pushed into the upper liquid whose dielectric constant is smaller. However, from Fig. 7(a) we also notice that for $\epsilon_L = 5$ and $\sin \theta'_c > 0.8$, and for $\epsilon_L = 50$ and $\sin \theta'_c > 0.3$, f_v is negative, implying that the particle in these two cases is pushed into the lower liquid whose dielectric constant is larger. In other words, if the particle center is located below the interface at a distance larger than a critical distance (whose value depends on ϵ_L), the particle is pushed further downwards; otherwise, the electrostatic force pushes the particle upwards. Therefore, in the presence of an electric field the interface acts as a barrier because it opposes the motion of the particles across the interface. The figure, however, also suggests, since the vertical force is largely positive, that the electric force pushes particles into the fluid whose dielectric constant is smaller provided the latter are able to cross the interface barrier. The figure also shows that for $\epsilon_L = 1.1$ the force is maximal when $\theta'_c = 0$ and that the angle θ'_c for which the force is maximal decreases with increasing ϵ_L.

Similarly, for $\epsilon_p = 0.5$, shown in Fig. 7(b), there is a critical value of θ'_c at which f_v changes sign, and the critical value of θ'_c decreases with increasing ϵ_L. This, as in Fig. 7(a), implies that the electrostatic force pushes the particle away from the flat interface, and thus, as it was the case above, the interface acts as a barrier for the particles. The critical value of θ'_c in Fig. 7(b), however, is smaller than in Fig. 7(a) at the
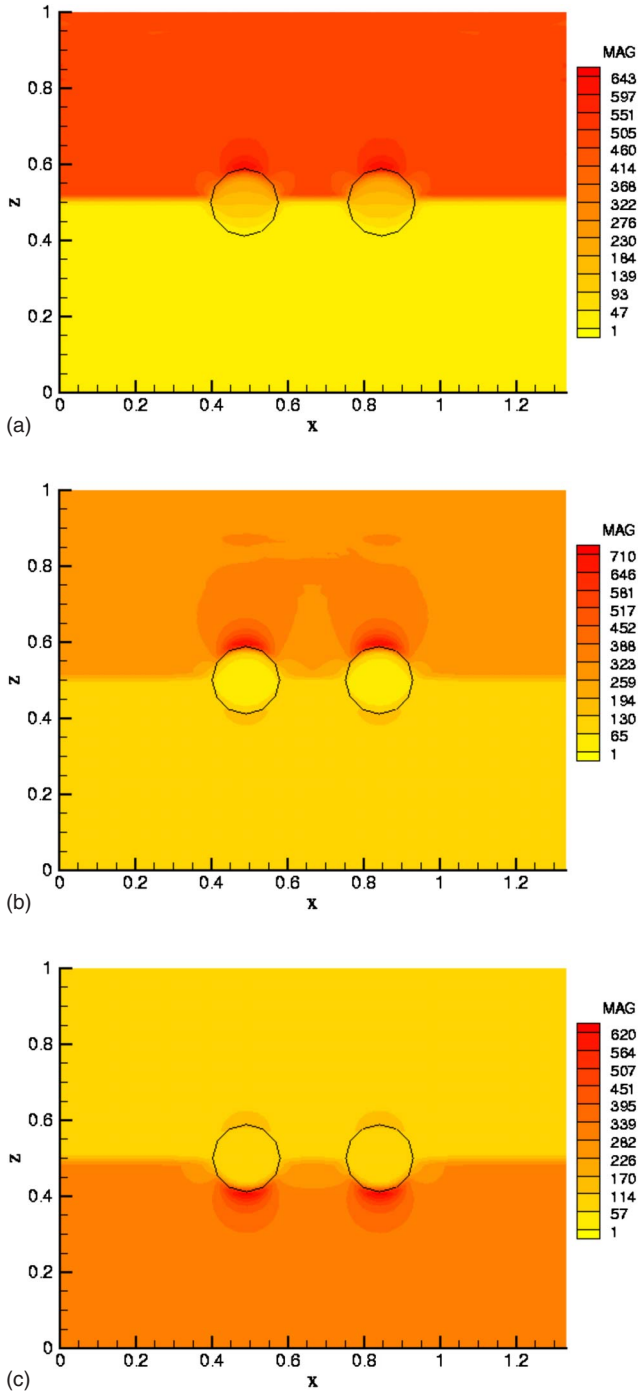
FIG. 4. (Color online) The electric field intensity on the domain midplane passing through the particles centers for the device shown in Fig. 2, for various dielectric constant values. The spherical particles of radius a are placed so that their centers are aligned with the nondeformed interface and at a distance $2.6a$ of each other. The spheres alter the electric field distribution, and experience an electrostatic force. The dielectric constants of the upper fluid, lower fluid, and the particles were set to (a) $\epsilon_a=1$, $\epsilon_L=5$, and $\epsilon_p=2$. The vertical force is 4.16 and the lateral force is -0.156, (b) $\epsilon_a=1$, $\epsilon_L=2$, and $\epsilon_p=5$. The vertical force is 3.39 and the lateral force is -0.34, (c) $\epsilon_a=1$, $\epsilon_L=5$, and $\epsilon_p=2$. The vertical force is -1.49 and the lateral force is -0.124. In all cases, the lateral electrostatic force is repulsive while the vertical electrostatic force can be either upward (a),(b) or downward (c).
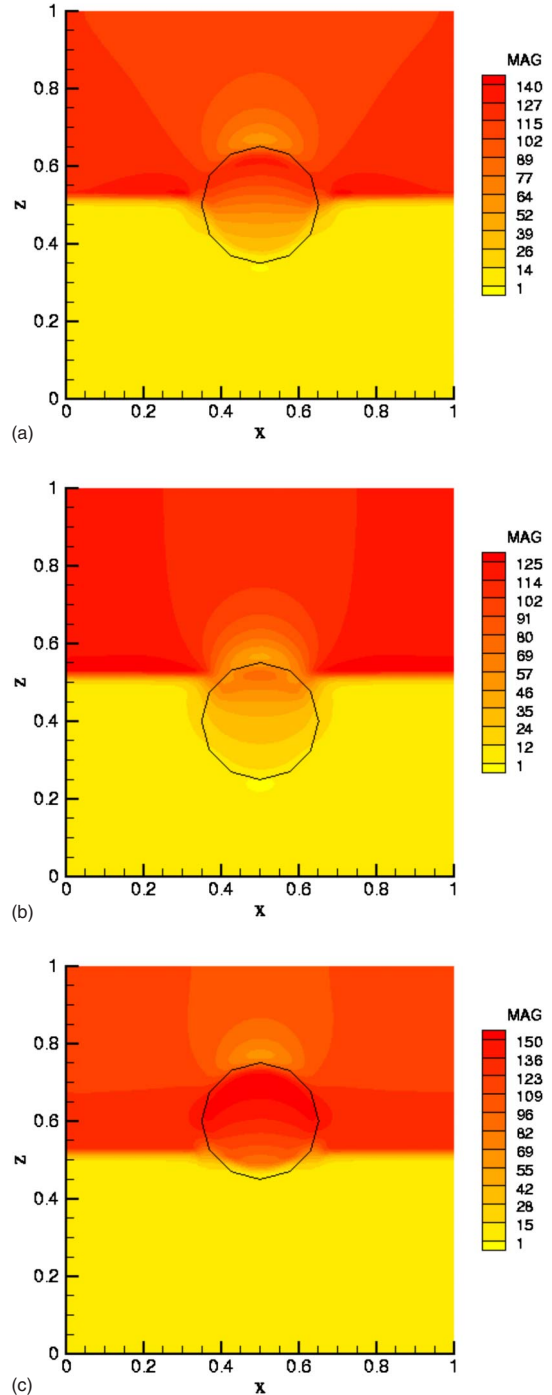
FIG. 5. (Color online) Electric field intensity on the domain midplane for the device shown in Fig. 2 in which one particle is placed at the interface. The dependence of the electric field upon the position of the particle within the interface is studied. The dielectric constants were set to $\epsilon_a=1$, $\epsilon_L=5$, and $\epsilon_p=0.5$. The particle alters the electric field distribution and experiences an electrostatic force in the vertical direction. The direction of the force, as well as its magnitude, depends on the particle position within the interface. (a) The sphere center is at the interface. The vertical electrostatic force is 0.354 (in the upward direction). (b) The sphere center is at a distance of $0.6a$ below the interface. The vertical electrostatic force is -2.22 (in the downward direction). (c) The sphere center is at a distance of $0.6a$ above the interface. The vertical electrostatic force is 0.553.
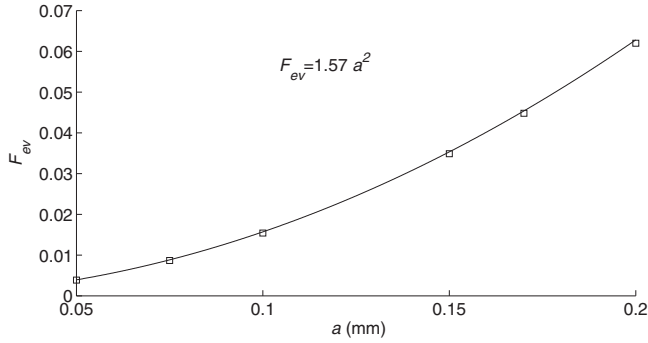
FIG. 6. The vertical electrostatic force computed numerically is plotted as a function of the particle radius a, along with the best power law fit, showing the quadratic dependence of the force on the particle radius. The dielectric constants were assumed to be $\epsilon_a=1$, $\epsilon_L=2$, and $\epsilon_p=1.5$.

same ϵ_L value. The actual vertical position (θ'_c) of a particle is, of course, determined by the balance of the buoyant weight, the vertical capillary force, and the electrostatic force.

C. Lateral electrostatic forces

The dipole-dipole interaction force between two dielectric spheres immersed in a fluid with the dielectric constant ϵ_a and subjected to a uniform electric field, in the point-dipole limit, is given by the following well-known expression in spherical coordinates [8,9]:

$$\mathbf{F}_D(r,\theta) = f_0 \left(\frac{a}{r}\right)^4 [(3\cos^2\theta - 1)\mathbf{e}_r + \sin 2\theta \ \mathbf{e}_\theta], \quad (2)$$

where $f_0 = 12\pi\epsilon_0\epsilon_a a^2\beta^2E^2$ (E being the magnitude of the uniform electric field along the z axis), θ denotes the angle between the z axis and the vector $\mathbf{r}$ joining the centers of the two particles, $r=|\mathbf{r}|$, $\beta=(\epsilon_p-\epsilon_a)/(\epsilon_p+2\epsilon_a)$ is the Clausius-Mossotti factor, and ϵ_p is the dielectric constant of the particle. If the electric field is perpendicular to the line joining the centers of the particles, i.e., $\theta=\pi/2$, the interaction force is repulsive and tangential to the interface.

However, the above expression is not applicable to particles floating in a two-fluid interface, as the fluid's dielectric constant changes discontinuously across the interface. The computations described above were used to show that the lateral interaction force can be written as

$$F_D(r) = \epsilon_0\epsilon_a\left(\frac{\epsilon_L}{\epsilon_a} + 1\right)a^2E^2\left(\frac{a}{r}\right)^4 f_D\left(\frac{\epsilon_L}{\epsilon_a}, \frac{\epsilon_p}{\epsilon_a}, \theta_c, \frac{h_2}{a}\right), \quad (3)$$

where f_D is a dimensionless function of the included arguments, with the force depending upon the sixth power of the particle radius a and on the fourth power of the inverse of the distance between the particles as shown in Fig. 8(a) and 8(b). As was the case for Eq. (1), the above expression is obtained by assuming that the interface is flat and that it intersects the sphere's surface at θ_c. The force also depends on the dielectric constants of the two fluids involved, and the positions θ_c of the particles within the interface. The latter in this study is assumed to be the same for the two particles. However, if
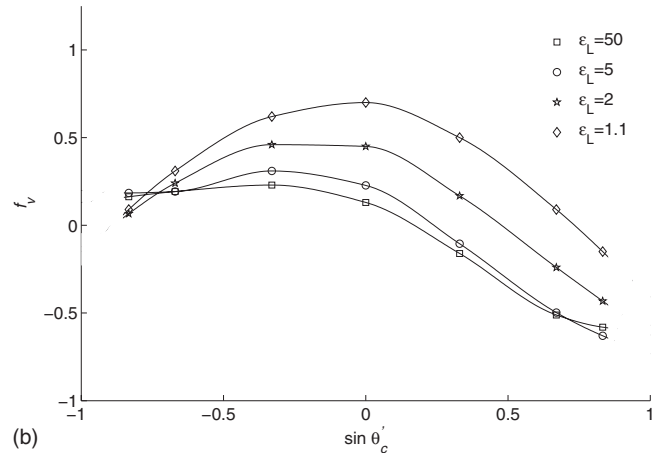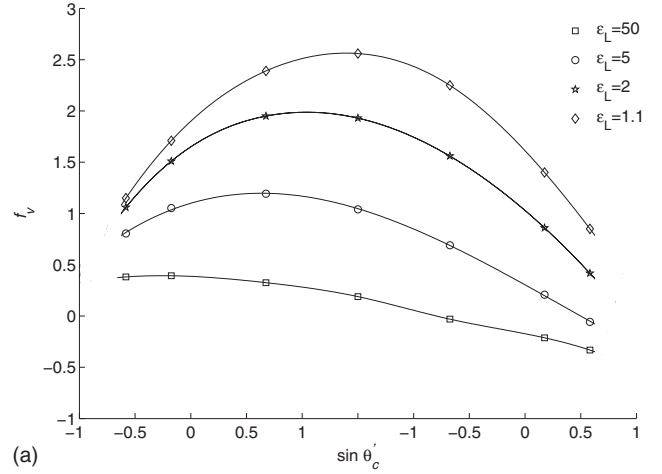

FIG. 7. The vertical electrostatic force coefficient f_v is plotted as a function of $\sin\theta'_c$ for $\epsilon_L=1.1$, 2, 5, and 50. The dielectric constant of the particle is 2.0 (a) and 0.5 (b) and that of the upper liquid is 1.0.

particles were not of the same type or size, their positions θ_c within the interface would be different, and the interaction force would be even more complex.

Figure 9 displays the force coefficient f_D as a function of $\sin\theta'_c$ for $\epsilon_a=1$, and $\epsilon_p=2.0$ [Fig. 9(a)] and 0.5 [Fig. 9(b)]. The force is repulsive for all values of ϵ_L investigated. From Fig. 9(a) we note that for $\epsilon_p=2.0$ and $\epsilon_L=50$, the magnitude of f_D is maximum when θ'_c is around zero, but is relatively independent of θ'_c for $\epsilon_L=1.1$ and 5.0. Also notice that for $\epsilon_L=2.0$, as expected, f_D goes to zero when the sphere is completely submerged in the lower liquid as, in this case, the dielectric constant of the particles is the same as that of the lower fluid.

For the case corresponding to $\epsilon_p=0.5$ shown in Fig. 9(b), f_D increases in magnitude with increasing θ'_c when $\theta'_c<0$ for $\epsilon_L=1.1$ and 2.0. This is due to the fact that the dielectric constant of the lower fluid is larger than that of the upper fluid. However, for $\epsilon_L=5$ and 50, f_D attains a maximum value in magnitude and then decreases with increasing θ'_c. This result suggests that for larger values of ϵ_L the interface enhances the repulsive force between the particles.
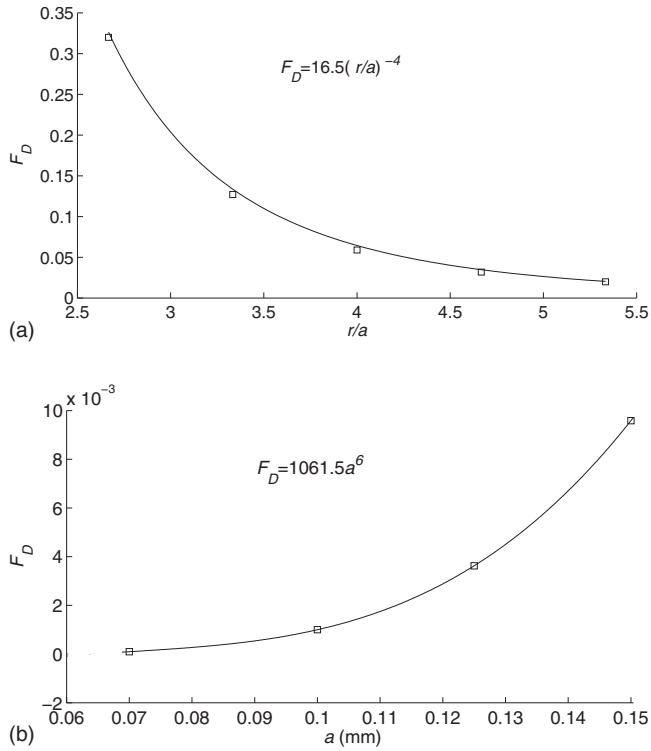
(a)

(b)

FIG. 8. The lateral dipole-dipole interaction force computed numerically is plotted as a function of (a) the dimensionless distance r/a between the particles and (b) the particle radius a for a fixed distance r between the particles. The best power law fits, showing that the force depends on the inverse of the fourth power of the distance between the particles and on the sixth power of the particle radius, are also shown. The dielectric constants are assumed to be $\epsilon_a=1$, $\epsilon_L=2$, and $\epsilon_p=1.5$.

The repulsive interaction energy W_D between two particles can be obtained by integrating Eq. (3) with respect to r, which gives

$$W_D(r) = -\frac{1}{3}\epsilon_0\epsilon_a\left(\frac{\epsilon_L}{\epsilon_a}+1\right)a^2E^2\left(\frac{a^4}{r^3}\right)f_D\left(\frac{\epsilon_L}{\epsilon_a},\frac{\epsilon_p}{\epsilon_a},\theta_c,\frac{h_2}{a}\right).$$
(4)

Let us assume that $\epsilon_a=2.0$, $\epsilon_L=4.0$, $E=3\times10^6$ volt/m, $f_D=3.1$, and $r=2a$. For these parameter values, the interaction energy is shown as a function of the particle radius in Fig. 10. For $a=1$ μm, $W_D(r)=\sim1.67\times10^4$ kT and for $a=100$ nm, $W_D(r)=\sim16.7$ kT, where k is the Boltzman constant and T is the temperature, indicating that the repulsive electrostatic force is larger than the random Brownian force acting on the particles. This shows that the electrostatic repulsive force (3) can be used to manipulate nanoparticles within a two-fluid interface.

D. Vertical force balance in equilibrium

We next consider the vertical force balance for a spherical particle floating within the interface between two immiscible fluids. The buoyant weight F_b of the particle is balanced by the capillary force F_c and the electrostatic force F_{ev}, that is
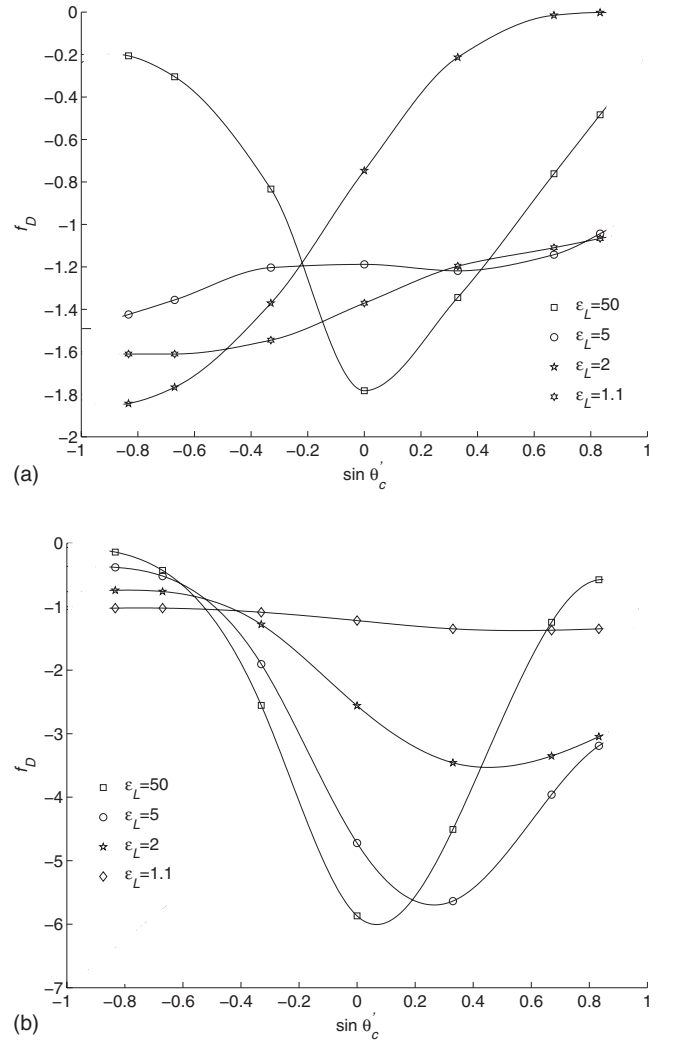

(a)

(b)

FIG. 9. The dipole interaction force coefficient f_D is plotted as a function of $\sin\theta_c'$ for $\epsilon_L=1.1$, 2, 5, and 50. The dielectric constant of the particle is 2.0 (a) and 0.5 (b) and that of the upper liquid is 1.0. The distance between the particles is $2.6a$.

$$F_c + F_{ev} + F_b = 0.$$
(5)

The buoyant weight is given by $F_b = -g\rho_L a^3 f_b(\rho_a/\rho_L, \rho_p/\rho_L, \theta_c, h_2/a)$, where g is the acceleration due to gravity, ρ_p is the particle density, ρ_a and ρ_L are the densities of the upper and lower fluids, θ_c and h_2 are defined in Fig. 2, and f_b is a function of ρ_a/ρ_L, ρ_p/ρ_L, θ_c and h_2/a. It is easy to deduce from Fig. 2 that the capillary force F_c takes the expression $F_c=-2\pi\gamma a\sin\theta_c\sin(\theta_c+\alpha)$, where α is the contact angle. Therefore, Eq. (5) can be rewritten as

$$F_c = -2\pi\gamma a\sin\theta_c\sin(\theta_c+\alpha)$$
$$= g\rho_L a^3 f_b\left(\frac{\rho_a}{\rho_L},\frac{\rho_p}{\rho_L},\theta_c,\frac{h_2}{a}\right)$$
$$-a^2\epsilon_0\epsilon_a\left(\frac{\epsilon_L}{\epsilon_a}-1\right)E^2 f_v\left(\frac{\epsilon_a}{\epsilon_L},\frac{\epsilon_p}{\epsilon_L},\theta_c,\frac{h_2}{a}\right).$$
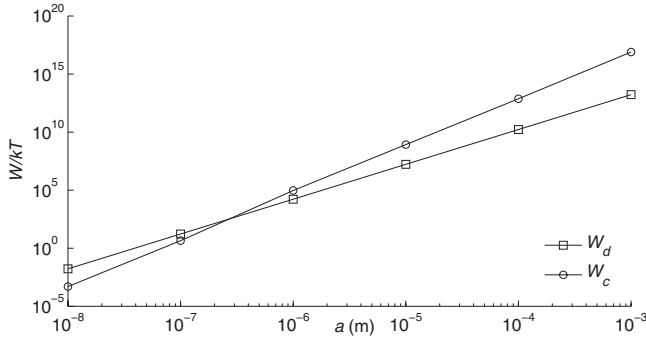(6a)

In dimensionless form, the previous equation reads

FIG. 10. Energies of capillary attraction (W_c) and dipole-dipole repulsion (W_d), in kT units, are plotted against the particle radius. For $W/(kT) > 1$, the capillary attraction and the dipole-dipole repulsion are stronger than the Brownian force for all particles sizes down to a radius of approximately 100 nm. The parameters are ϵ_a =2.0, ϵ_L=4.0, $E=3 \times 10^6$ volt/m, f_v=1, f_D=1, γ=0.01, ρ_a =1 kg/m^3, ρ_L=1000, ρ_p=3000 kg/m^3, and $r=2a$.

$$2\pi \sin \theta_c \sin(\theta_c + \alpha) = -B\; f_b\left(\frac{\rho_a}{\rho_L}, \frac{\rho_p}{\rho_L}, \theta_c, \frac{h_2}{a}\right)$$
$$+ W_E\left(\frac{\epsilon_L}{\epsilon_a} - 1\right) f_v\left(\frac{\epsilon_a}{\epsilon_L}, \frac{\epsilon_p}{\epsilon_L}, \theta_c, \frac{h_2}{a}\right). \tag{6b}$$

Here $B = \rho_L a^2 g/\gamma$ is the Bond number and $W_E = \epsilon_0 \epsilon_a a E^2/\gamma$ is the electric Weber number.

As the particle radius a approaches zero, the Bond number $B = \rho_L a^2 g/\gamma \rightarrow 0$. In this limit, in the absence of an electrostatic force, the right hand side of Eq. (6b) is zero and thus $\sin(\alpha + \theta_C) \approx 0$ or $\theta_C \approx \pi - \alpha$ (see Fig. 2). This means that a small particle floats so that the interfacial deformation is insignificant. Hence, the lateral capillary force, which arises from the interfacial deformation, in this limit, is also insignificant. As noted earlier, for particles floating on water, this limit is reached when the particles radius is approximately 10 μm (see Ref. [3]).

Another important limit is the case for which the Bond number approaches zero, but W_E does not. This situation arises, for instance, for small particles when the magnitude of the electric field is sufficiently large. The equilibrium position of a particle within the interface in this case is determined by the balance of the interfacial and electrostatic forces alone. The interface is then deformed by the particle, and so the lateral (electric field induced) capillary forces are present and can cause particles within the interface to cluster.

E. Interfacial deformation and lateral capillary force

In equilibrium, the external vertical force acting on a particle is balanced by the vertical component of the capillary force which, as noted earlier, arises because of the deformation of the interface. The profile of the deformed interface around a particle can be obtained by integrating Laplace's equation and using the boundary conditions that (i) the interface far away from the particle is flat and (ii) the angle between the interface and the horizontal at the particle surface is known in terms of the total external force acting on the

particle. It can be shown that the interface height $\eta(r)$ at a distance r from a spherical particle is given by (see Refs. [3,5,10])

$$\eta(r) = a \sin(\theta_c + \alpha) K_0(qr), \tag{7}$$

where $K_0(qr)$ is the modified Bessel function of zeroth order and $q = \sqrt{(\rho_L - \rho_a)g/\gamma}$. In obtaining the above expression we have ignored the influence of the electrostatic stress on the interface, including the stress that arises due to the presence of the particle, and assumed that the interfacial deformation is small.

Let us consider a second particle at a distance r from the first particle. The height of the second particle is lowered because of the interfacial deformation caused by the first particle, and thus the work done by the electrostatic force and gravity (buoyant weight) is

$$W_c = \eta(r)(F_{ev} + F_b). \tag{8}$$

Notice that the electrostatic force is due to a field that is external to the fluid-particle system, as is the gravitational field, and therefore the work done by both fields is treated in a similar manner. In this analysis, we will ignore the work done by the electrostatic stress that acts on the two-fluid interface. In addition, this analysis of the behavior of two particles does not account for the multi body interactions. Using Eqs. (6a), (6b), and (7), Eq. (8) can be rewritten as

$$W_c = -\frac{(F_{ev} + F_b)^2}{2\pi\gamma} K_0(qr)$$
$$= -\left[-\epsilon_0 \epsilon_a\left(\frac{\epsilon_L}{\epsilon_a} - 1\right) a^2 E^2 f_v + \frac{4}{3}\pi a^3 \rho_p g f_b\right]^2 \frac{1}{2\pi\gamma} K_0(qr). \tag{9}$$

In Fig. 10, the interaction energy W_c due to the lateral capillary force is plotted as a function of the particle radius. The parameter values are ϵ_a=2.0, ϵ_L=4.0, $E=3 \times 10^6$ volt/m, f_v=1, γ=0.01, ρ_a=1 kg/m^3, ρ_L=1000 kg/m^3, ρ_p =3000 kg/m^3, and $r=2a$. The figure shows that for these parameter values, the interaction energy (9) is significant for nanosized particles.

The lateral capillary force between two particles is therefore given by

$$F_{lc} = -\frac{dW_c}{dr}$$
$$= \left[-\epsilon_0 \epsilon_a\left(\frac{\epsilon_L}{\epsilon_a} - 1\right) a^2 E^2 f_v + \frac{4}{3}\pi a^3 \rho_p g f_b\right]^2 \frac{qK_1(qr)}{2\pi\gamma}, \tag{10}$$

where $K_1(qr)$ is the modified Bessel function of first order. When the two particles are far away from each other, the above reduces to

$$F_{lc} = -\left[-\epsilon_0\epsilon_a\left(\frac{\epsilon_L}{\epsilon_a} - 1\right)a^2 E^2 f_v + \frac{4}{3}\pi a^3 \rho_p g f_b\right]^2 \frac{1}{2\pi\gamma\, r}.$$

(11)

Notice that the lateral capillary force depends on the net vertical force acting on the particle, which includes its buoyant weight and the vertical electrostatic force. The force varies as the fourth power of the applied electric field and if the electrostatic force and the buoyant weight are in the same direction, the electric field enhances the lateral capillary forces among the particles.

However, it is noteworthy that the vertical electrostatic force may not be in the same direction as the buoyant weight, and if this is the case there is a critical value of the electric field strength for which the net vertical force acting on the particle is zero. The lateral capillary force among the particles under these conditions would also be zero; this suggests that the electric field can be used to decrease, or even eliminate, capillarity induced attraction among the particles. If the electric field strength is increased further, the particles move upward in the interface and the capillary forces arise again but the interface near the particles would be curved downwards. Here we wish to note that the capillary force can cause particles to interact with each other only when the associated interaction energy is greater than kT, and therefore when the net external vertical force acting on the particles is small the latter are not likely to cluster as their motion would be governed by thermal fluctuations.

F. Spacing between particles

The dimensionless equilibrium separation $r_{eq}/(2a)$ between two particles can be obtained by equating the repulsive electrostatic force (3) and the above attractive capillary force (11). After simplification, we obtain

$$\frac{r_{eq}}{2a} = \frac{1}{2}\left(\frac{2\pi\epsilon_0\epsilon_a\left(\frac{\epsilon_L}{\epsilon_a} + 1\right)\gamma E^2 f_D}{a\left[-\epsilon_0\epsilon_a\left(\frac{\epsilon_L}{\epsilon_a} - 1\right)E^2 f_v + \frac{4}{3}\pi a\rho_p g f_b\right]^2}\right)^{1/3}.$$

(12)

This expression gives the dependence of $r_{eq}/(2a)$ on the parameters of the problem. However, we remind the reader that the dimensionless parameters f_v, f_D, and f_b themselves depend on several parameters [this dependence is not reproduced in Eq. (12) for the sake of simplicity]. Notice that $r_{eq}/(2a)$ decreases with increasing particle radius a.

We now consider two limiting cases of the previous expression. The first is the case of relatively large particles for which the buoyant weight is much larger than the vertical electrostatic force. In this situation, Eq. (12) implies that $r_{eq}/(2a)$ increases with increasing electric field strength as $E^{2/3}$. This is approximately the case for $a = 10^{-3}$ m, as shown in Fig. 11(a). These conclusions are in agreement with the experimental data reported in Ref. [1] for particles with $r = \sim 10^{-3}$ m. The attractive capillary forces for such particles

primarily originate in the interfacial deformation due to their buoyant weight, and the repulsive force is due to the dipole-dipole interaction between them.

The second limiting case is that of relatively small sized particles for which the buoyant weight is negligible compared to the vertical electrostatic force. From Eq. (12), after the buoyant weight is neglected, we obtain that $r_{eq}/(2a)$ decreases with increasing electric field strength as $E^{-2/3}$. As shown in Fig. 11(b), this limiting case is approximately reached for $a = 1$ μm. Both attractive and repulsive forces in this case are due to the applied electric field (since the buoyant weight is negligible). The attractive part varies as the fourth power of the electric field, but is long ranged (varies as r^{-1}). The repulsive part, on the other hand, varies as the square of the electric field, but is short ranged (varies as r^{-4}).

Here we wish to distinguish the above result with the model presented in Ref. [11] to explain the observation that small charged particles within an interface between water and a nonpolar liquid, such as air or oil, form periodic arrangements. They showed that in addition to interacting electrostatically with each other, the charged particles experience lateral capillary forces that arise because of the deformation of the interface (also see Ref. [12]). The interfacial deformation in this case is not due to the particles weight (which is negligible) or an externally applied electric field (which is the case discussed in this paper), but due to a vertical electrostatic force that acts on the particle within the interface because of its charge.

In the intermediate range between the two previous limiting cases, the attractive capillary force is a result of the net vertical force acting on the particles, which includes both the buoyant weight and the vertical electrostatic force. In an actual physical system, this intermediate range correspond to particle radii between ~ 10 and ~ 100 μm. We now consider first the case in which the electrostatic force and the buoyant weight are in the same direction. The latter dominates when the electric field strength is small, and therefore, the distance between the particles increases with increasing electric field [see Fig. 11(c)]. However, as the electric field strength is increased to a level where the vertical electrostatic force is much larger than the buoyant weight, the distance between the particles decreases with increasing electric field strength. Here, it is important to note that this result can be observed in experiments only if the electrostatic and capillary forces are larger than the Brownian forces. Furthermore, the former forces cannot be observed if they do not cause an observable deterministic motion. This may be the case if the distance between the particles is too large.

We next consider the case in which the electrostatic force and the buoyant weight are not in the same direction. In this case, there is a critical value of the electric field strength at which the lateral capillary force is zero. This corresponds to the situation where the sum of the buoyant weight and the vertical electrostatic force on the particle is zero. As a result, as shown in Fig. 11(d), $r_{eq}/(2a)$ approaches infinity because the only lateral force the particles experience is the repulsive electrostatic force. However, since the repulsive electrostatic force decays as the fourth power of the distance between the particles, in experiments, the particles are expected to move only to a distance at which the associated interaction energy
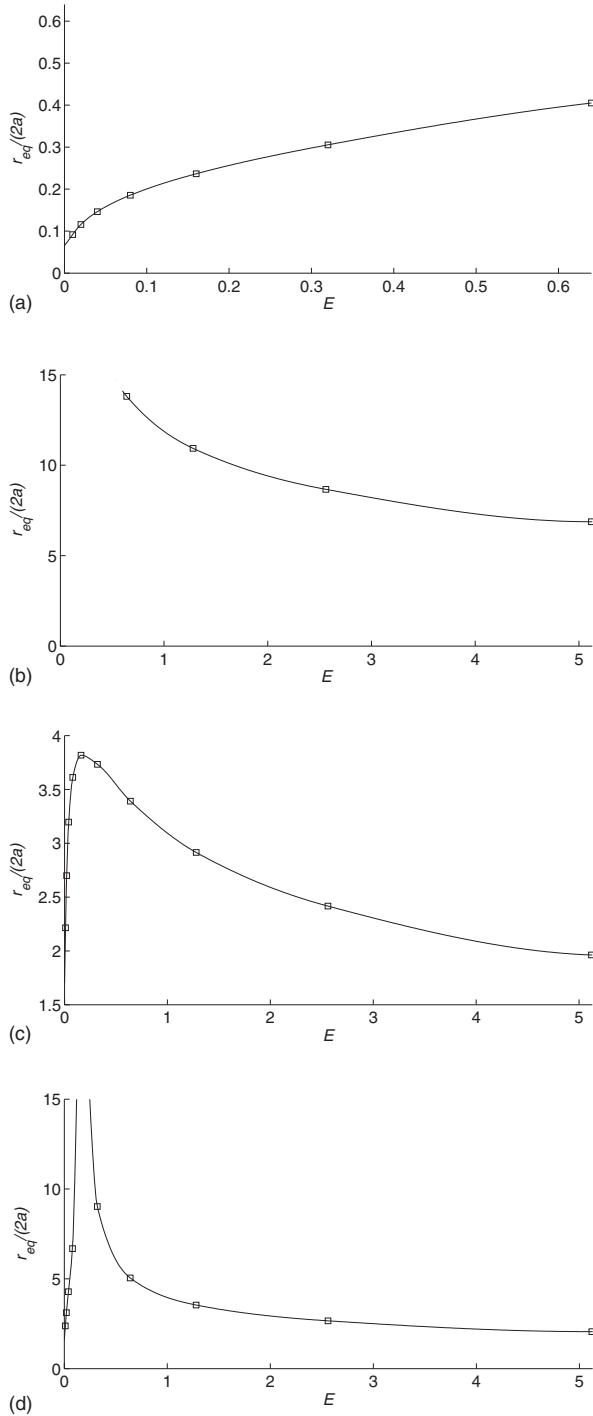
FIG. 11. The dimensionless equilibrium separation between two particles is plotted as a function of E for three values of the particle radius a. (a) $a=10^{-3}$ m, $r_{eq}/(2a)$ increases with increasing E. (b) $a=1$ μm, $r_{eq}/(2a)$ decreases with increasing E. (c) The buoyant weight and the vertical electrostatic force are in the same direction and $a=4\times10^{-5}$ m. For E small, $r_{eq}/(2a)$ increases with increasing E, but for E large it decreases with increasing E. (d) The buoyant weight and the vertical electrostatic force are in the opposite directions and $a=4\times10^{-5}$ m. For small values of E, $r_{eq}/(2a)$ increases with increasing E. There is a critical value of E for which the lateral capillary force is zero and thus particles only experience the repulsive electrostatic force and $r_{eq}/(2a)$ approaches infinity. For E large, $r_{eq}/(2a)$ decreases with increasing E.

becomes comparable to kT. Another interesting feature of the curve in Fig. 11(d) is that a further increase of the electric field strength causes the lateral capillary forces to increase (since the sum of the buoyant weight and the vertical electrostatic force on the particle is again nonzero) and $r_{eq}/(2a)$ to decrease.

III. DISCUSSION AND CONCLUSIONS

In view of explaining in detail the clustering of particles reported experimentally in Ref. [1], we have studied the electrostatic and capillary forces acting on a particle within a two-fluid interface in the presence of both an externally applied electric field and other particles. Specifically, we have determined the dependence of the electrostatic force upon the dielectric properties of the fluids and the particles, as well as the position of the particle within the interface. It was assumed that the particles and the two fluids involved are perfect dielectrics, and that the particles are spherical. The electrostatic force was found to contain components both normal and tangential to the interface. The former arises because the dielectric constants of the two fluids involved are different and the latter is due to the dipole-dipole interactions among the particles. The component of the electrostatic force normal to the interface is shown to vary as the square of the particle radius a^2. For sufficiently large distances between the particles, the lateral electrostatic force between two particles varies as a^6 and decreases with increasing distance between the particles as r^{-4}. We have also shown that when $E\sim 3\times10^6$ V/m, the electrostatic forces can be used to manipulate the distance between nanosized particles floating at a two-fluid interface. Expressions of the various forces involved, as well as the equilibrium distance between the particles were given in Ref. [1], with a reference to the present paper for details.

The normal component of the electrostatic force, including its sign, depends on the dielectric constants of the fluids and particles. The equilibrium particle position θ_c of a particle within the interface is determined by the balance of the buoyant weight, the vertical interfacial force and the vertical electrostatic force. For small spherical particles, in the absence of an electric field the particle's position is primarily determined by the contact angle since the buoyant weight is negligible. Our numerical results show that when the dielectric constant of the upper fluid is smaller than that of the lower fluid and the particle's center is above the undeformed interface (this is the case for a small particle which is non-wetting with the lower liquid), the electrostatic force is in the upward direction. If, on the other hand, the particle center is below the undeformed interface (this is the case for a small particle which wets the lower liquid), there is a critical value of θ_c at which the electrostatic force changes direction. The critical value of θ_c depends on the dielectric constants of the fluids and the particle. Therefore, in the presence of an externally applied electric field, the interface acts like a barrier to the particles: the electrostatic force pushes the particles below the interface downwards and those above the interface upwards. The overall tendency of the electric force, however, is to push particles into the fluid region whose dielectric

constant is smaller, but this can occur only if the particles have sufficient energy to cross the electric interface barrier.

In equilibrium, the net vertical force acting on a particle at the interface, which includes the electrostatic force and the buoyant weight, is balanced by the vertical capillary force which arises because of the deformation of the interface. The deformation of the interface, in turn, gives rise to lateral capillary forces which cause particles at the interface to cluster. More specifically, it is shown that the magnitude of these lateral forces is determined by the square of the net vertical force acting on the particle which includes both the buoyant weight and the vertical electrostatic force. The lateral capillary forces are long ranged and depend on the fourth power of the electric field intensity.

The buoyant weight and the vertical electrostatic force, however, may not be in the same direction, and when this is the case the electric field, in fact, reduces lateral capillary forces. If the electrostatic force and buoyant weight are in the same direction, the electric field enhances lateral capillary forces. This is an important result, especially for micron and sub micron sized particles for which the buoyant weight is negligible, because it shows that the clustering behavior of particles, including that of small particles, can be controlled using an externally applied electric field.

The equilibrium distance between two particles was obtained by equating the attractive capillary and repulsive electrostatic forces. Equilibrium is possible because the attractive capillary force between the particles is long ranged (decays as r^{-1}) and dominates the electrostatic repulsive force which is short ranged (decays as r^{-4}) when the distance between the particles is large. The opposite is true when the distance between the particles is small. The equilibrium distance was shown to depend on the particle radius, the electric field intensity, the buoyant weight, the particle's position within the interface and the dielectric constants. These results are in agreement with the recent experiments reported in Ref. [1] which show that the equilibrium distance between particles can be controlled by adjusting the electric field strength (see Fig. 1).

The theoretical results presented here correctly capture the trends observed in experiments. For example, the variation of the dimensionless equilibrium distance $r_{eq}/(2a)$ between two particles with the electric field strength, and also with the particle radius is predicted correctly as shown in
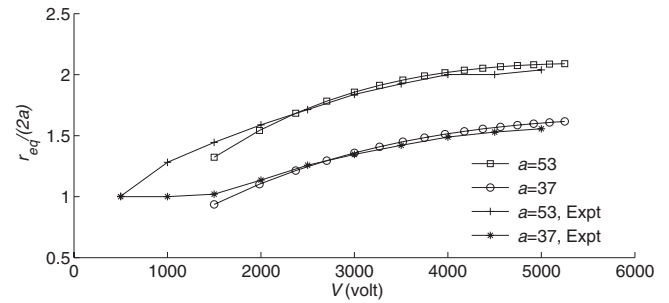

FIG. 12. The equilibrium separation $r_{eq}/(2a)$ between two particles for $a=37$ and 53 μm as given by Eq. (12) and the actual measured values (denoted by "expt.") are shown as functions of the voltage applied to the device described in Ref. [1]. The electric force coefficients were numerically estimated to be $f_v=0.27$, $f_D=0.019$, and $f_b=0.64$. From the experimental photographs, we estimated $\theta_c=76.5°$ for the particles with $a=37$ μm, and this value was used for both cases. The agreement between the theory and the experimental data is very good, especially when the distance between the particles is more than $2.5a$, considering that there are no adjustable parameters.

Fig. 12. The figure displays $r_{eq}/(2a)$ given by Eq. (12), along with the actual measured values, as functions of the voltage applied to the device described in Ref. [1]. The data is presented for $a=37$ and 53 μm. The distance between two particles increases with increasing electric field and with decreasing particle radius. From Sec. II F we know that in the limiting cases the dimensionless distance between two particles varies as E^β. For relatively large sized particles ($a > \sim 1000$ μm), for which the buoyant weight dominates, $\beta=2/3$, and for submicron sized particles, $\beta=-2/3$. For the data presented in Fig. 12, the distance between the particles increases with increasing E. According to Eq. (12), for submicron sized particles the distance between two particles should decrease with increasing electric field strength. At present, such experimental data for micron and submicron sized particles is not available, and therefore we are unable to verify the predictions of our theory for this size range. This reversal in the particle separation with increasing electric field strength, as noted before, is a consequence of the fact that the attractive capillary force is not a result of the particles' buoyant weight, but instead arises from the vertical electric force acting on the particles.

[1] N. Aubry, P. Singh, M. Janjua, and S. Nudurupati, Proc. Natl. Acad. Sci. U.S.A. **105**, 3711 (2008).

[2] N. Aubry and P. Singh, *International Mechanical Engineering Congress and Exposition (IMECE) Proceedings* (ASME, New York, 2007), paper No. 2007–44095.

[3] M. A. Fortes, Can. J. Chem. **60**, 2889 (1982); W. A. Gifford and L. E. Scriven, Chem. Eng. Sci. **26**, 287 (1971); P. A. Kralchevsky, V. N. Paunov, N. D. Denkov, I. B. Ivanov, and K. Nagayama, J. Colloid Interface Sci. **155**, 420 (1993); J. Lucassen, Coll. Surf. **65**, 131 (1992); P. Singh and D. D. Joseph, J. Fluid Mech. **530**, 31 (2005).

[4] N. Bowden, I. S. Choi, B. A. Grzybowski, and G. M. Whitesides, J. Am. Chem. Soc. **121**, 5373 (1999); N. A. Bowden, A. Terfort, J. Carbeck, and G. M. Whitesides, Science **276**, 233 (1997); B. A. Grzybowski, N. Bowden, F. Arias, H. Yang, and G. M. Whitesides, J. Phys. Chem. B **105**, 404 (2001).

[5] P. A. Kralchevsky and K. Nagayama, Adv. Colloid Interface Sci. **85**, 145 (2000).

[6] D. Y. C. Chan, J. D. Henry, Jr., and L. R. White, J. Colloid Interface Sci. **79**, 410 (1981); D. Stamou and C. Duschl, Phys. Rev. E **62**, 5263 (2000).

[7] J. Kadaksham, P. Singh, and N. Aubry, J. Fluids Eng. **126**, 170

(2004); Electrophoresis **25**, 3625 (2004); **26**, 3738 (2005); Mech. Res. Commun. **33**, 108 (2006); N. Aubry and P. Singh, Europhys. Lett. **74**, 623 (2006).

[8] H. A. Pohl, *Dielectrophoresis* (Cambridge University Press, Cambridge, 1978); T. B. Jones, *Electromechanics of Particles* (Cambridge University Press, Cambridge, 1995); F. Mugele and J. Baret, J. Phys.: Condens. Matter **17**, R705 (2005).

[9] D. J. Klingenberg, S. Van Swol, and C. F. Zukoski, J. Chem. Phys. **91**, 7888 (1989); W. R. Smythe, *Static and Dynamic Electricity*, 3rd ed. (McGraw-Hill, New York, 1968).

[10] M. M. Nicolson, Proc. Cambridge Philos. Soc. **45**, 288 (1949).

[11] M. G. Nikolaides, A. R. Bausch, M. F. Hsu, A. D. Dinsmore, M. P. Brenner, C. Gay, and D. A. Weiz, Nature (London) **420**, 299 (2002).

[12] L. Foret and A. Wurger, Phys. Rev. Lett. **92**, 058302 (2004); R. Aveyard, B. P. Binks, J. H. Clint, P. D. I. Fletcher, T. S. Horozov, B. Neumann, V. N. Paunov, J. Annesley, S. W. Botchway, D. Nees, A. W. Parker, A. D. Ward, and A. N. Burgess, *ibid.* **88**, 246102 (2002); K. D. Danov and P. A. Kralchevky, J. Colloid Interface Sci. **298**, 213 (2006).